

Modeling the Spectra of Dense Hydrogen Plasmas: Beyond Occupation Probability

T. A. Gomez,^{1,2} M. H. Montgomery¹, T. Nagayama², D. P. Kilcrease³, and D. E. Winget¹

¹*Department of Astronomy, University of Texas, Austin, Texas 78712, USA; gomezt@astro.as.utexas.edu*

²*Sandia National Laboratories, Albuquerque, New Mexico 87185, USA*

³*Los Alamos National Laboratories, Los Alamos, New Mexico 87545, USA*

Abstract. Accurately measuring the masses of white dwarf stars is crucial in many astrophysical contexts (e.g., asteroseismology and cosmochronology). These masses are most commonly determined by fitting a model atmosphere to an observed spectrum; this is known as the spectroscopic method. However, for cases in which more than one method may be employed, there are well known discrepancies between masses determined by the spectroscopic method and those determined by astrometric, dynamical, and/or gravitational-redshift methods. In an effort to resolve these discrepancies, we are developing a new model of hydrogen in a dense plasma that is a significant departure from previous models. Experiments at Sandia National Laboratories are currently underway to validate these new models, and we have begun modifications to incorporate these models into stellar-atmosphere codes.

1. Astrophysical Context

White dwarf stars are of critical importance in many contexts, from defining the initial-final mass relation of low and intermediate mass stars (e.g., Catalán et al. 2008; Williams et al. 2009) to acting as independent chronometers for different components of the Galaxy (e.g., Winget et al. 1987; García-Berro et al. 2010).

For all of these investigations we require accurate estimates of the masses and temperatures of these stars. By far the most widely used technique, termed the “spectroscopic method”, involves fitting a model atmosphere to an observed spectrum of a star, and varying the T_{eff} and $\log g$ values to match the width and intensities of the spectral lines (Barstow et al. 2005), and optionally the continuum as well. The set of best-fit parameters are then identified as estimates of the temperature and surface gravity of the white dwarf.

2. Sources of Uncertainty

Problems in applying this method can arise from many sources of uncertainty: surface composition, the physics of convection, atomic physics, magnetic fields, etc. Recently, progress has been made on the effect of convection on the parameters derived

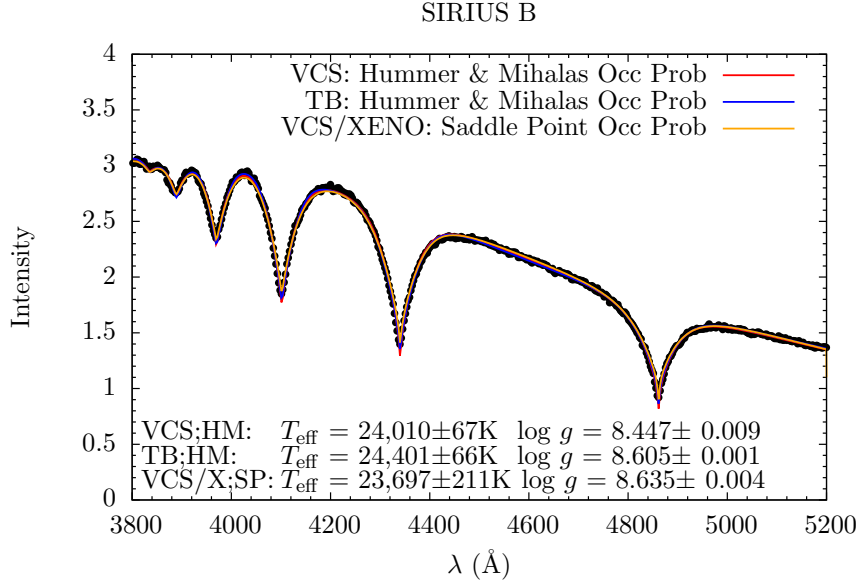


Figure 1. Three fits to a spectrum of Sirius B (HST STIS). The differences in derived parameters for each fit are due solely to the different assumed atomic physics of line profiles and the occupation probability of atomic states.

from spectroscopic fits of white dwarfs (e.g., Tremblay et al. 2011, 2013), but the other sources of uncertainty remain.

As an illustration of this, in Figure 1 we show three different fits to a spectrum of Sirius B (Barstow et al. 2005). All the fits reproduce the spectrum quite well but derive different estimates for the T_{eff} and $\log g$ of the star. The same model-atmosphere code *Tlusty* (Hubeny et al. 1994; Hubeny & Lanz 1995) was used to compute these fits; the only differences arose from the treatment of the atomic physics of line profiles and the occupation probability (OP) of atomic states. *Tlusty* includes OP put forth by Dappen et al. (1987) and Hummer & Mihalas (1988). The Hummer & Mihalas (1988) OP defines the ionization threshold by the Inglis & Teller (1939) criteria. However, there are other studies that show different ionization criteria (Luc-Koenig & Bachelier 1980). We therefore calculated model spectra with a different ionization criteria (defined by the saddle point in the potential) to compare the possible uncertainties in the $\log g$ (yellow line in Fig 1).

To resolve this discrepancy we would hope to appeal to independent techniques for determining Sirius B’s parameters. Unfortunately, astrometric and gravitational-redshift techniques disagree with each other, and with the spectroscopic method (e.g., Barstow et al. 2015). Thus, the time seems ripe to re-visit the physics of line formation in white dwarf atmospheres.

3. New Line-Profile Calculations

For an isolated atom, the atomic structure can often be calculated quite accurately. This is certainly the case for the hydrogen atom, since both the Schrödinger and Dirac

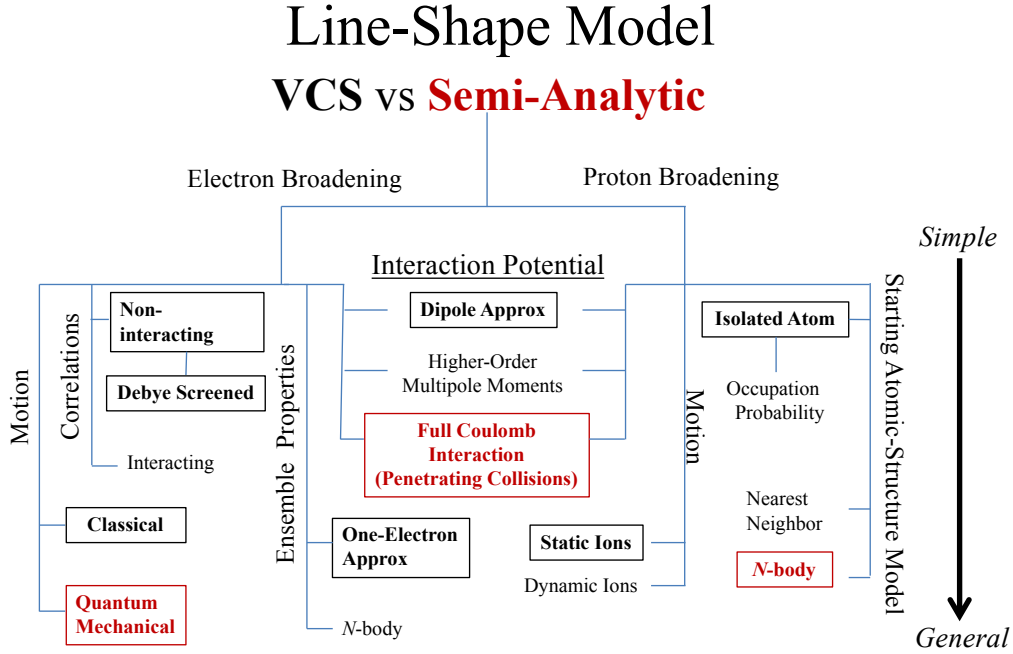


Figure 2. The “Approximation Tree” for the theory of line-profile modeling. The black, and bold-faced text boxes show the approximations used in the original VCS theory (Vidal et al. 1973), and the corresponding red, bold-faced items show the approximations used in our new semi-analytic approach.

equations have exact solutions. On the other hand, if the atom is embedded in a plasma, then it inherently becomes a many-body problem, and solutions are possible only within a set of approximations and methods.

In Figure 2, we depict the various approximations and approaches commonly used in line-profile calculations. The black, and bold-faced text boxes correspond to the approximations adopted by Vidal et al. (1973) and are commonly termed “VCS theory”, while the red, bold-faced text boxes show the set of approximations used in our new “semi-analytic” theory. We note that the recent improved line-profile calculations of Tremblay & Bergeron (2009) are essentially VCS theory plus the Hummer & Mihalas (1988) and Seaton (1990) formalism for treating continuum lowering and level dissolution. Hummer & Mihalas (1988) and Seaton (1990) define an ionization criteria for a given energy level, then perform a statistical average over plasma electric fields to determine the probability that the state is still “occupied”; this is known as occupation probability.

We have begun a program to re-examine the approximations shown in Figure 2 with an eye to which ones can be improved. To date, we have employed two approaches to this problem: 1) a simulation-based (*N*-body) approach, and 2) a semi-analytic approach. The simulation approach treats the perturbing influences of the protons and electrons classically and then solves the time-dependent Schrödinger equation numerically to obtain the broadened profiles. The semi-analytic approach treats the perturbing electrons quantum mechanically (Baranger 1958; Fano 1963, Gomez et al., in prep) and then solves the time-independent Schrödinger equation for the hydrogen atom in

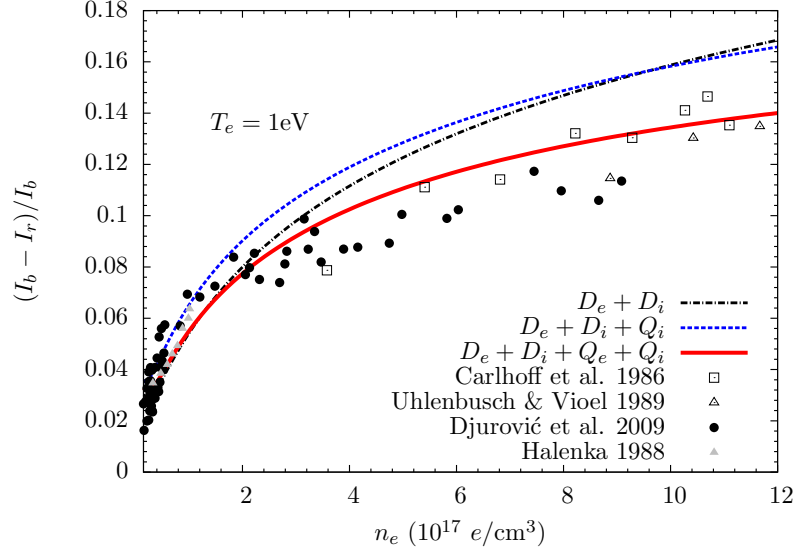


Figure 3. The red/blue asymmetry of $H\beta$ as a function of density (taken from Gomez et al. 2016). In the legend, D_e and Q_e indicate the dipole and quadrupole terms due to electrons, respectively, and similarly for the ions (D_i and Q_i). As indicated, the data (different style points) are taken from Carlhoff et al. (1986), Djurović et al. (2009), and Uhlenbusch & Vioel (1989).

the presence of several nearby protons. Both methods are able to explore different approximations and physical effects. For instance, we have used the simulation approach to explore ion dynamics (not discussed here; see Ferri et al. 2014, for more details) and the importance of higher-order multipoles (e.g., Gomez et al. 2016) of the interaction potential. We will use the semi-analytic approach to examine the importance of a quantum treatment of electrons and an ab initio treatment of continuum lowering (Crowley 2014).

3.1. Higher-order Multipole Moments

We have recently published results that improve the treatment of the electrostatic interaction potential. In Gomez et al. (2016), we use a simulation method to examine the importance of the higher-order terms in the multipole expansion of the interaction potential and the validity of the dipole approximation. While most calculations include only the dipole term, corresponding to a spatially constant electric field, we explored the effect which including higher-order gradients in the field (the quadrupole, octupole, and sedecapole terms) had on the detailed line-profile shape. For electron densities up to 10^{18} e/cc, we found that it was necessary to retain up to the quadrupole terms for both electrons and ions in the multipole expansion to correctly infer the density to within a few percent. In addition, these higher-order terms allowed us to match the height asymmetry seen in the “red” and “blue” central peaks of $H\beta$ (solid line in Figure 3). This is the first time that a theoretical calculation has been able to match this asymmetry for densities of $\sim 10^{17}$ – 10^{18} e/cc. While this feature is not usually seen in white dwarf spectra, it can be used as a density diagnostic for laboratory plasmas (Djurović et al. 2009).

3.2. *N*-body Treatment of Protons & Quantum Electrons

The red text boxes in Figure 2 show the approximations used in our semi-analytic approach. It differs from VCS (or TB) in that it: 1) has a *quantum* treatment of the perturbing electrons, 2) uses a full Coulomb interaction of the perturbing electrons with the radiating-atom wave function, including penetrating collisions, and 3) computes an exact numerical solution of the Schrödinger equation in the *N*-body potential of the nearby ions.

At high densities, the electric fields of nearby protons cause the energy levels of the radiating atom to begin to cross; this is termed the “Inglis-Teller limit” (Inglis & Teller 1939). The current reasoning (Hummer & Mihalas 1988) is that when energy levels cross, then the state is considered dissolved into the continuum. Preliminary results for the proton-dependent energy-level structure show that discrete states exist beyond the Inglis-Teller limit, but, due to the averaging of the different proton configurations and the electron broadening, the spectrum appears featureless above this threshold. This approach produces a different spectral shape for lines near the continuum compared to the standard treatment; this could result in systematically different inferred masses for white dwarf stars.

4. Discussion

We do not yet have results for the calculations using the approach described in section 3.2. As an illustration, however, in Figure 4 we show a comparison of a preliminary calculation using our semi-analytic model with the results of VCS and TB models.

Our new *N*-body atomic-structure calculation reveals many discrete states between 2.9 and 3.0 eV. However, when an average is taken over different free-proton configurations, these transitions are no longer discernible and the spectrum appears to be continuous. This direct treatment of proton perturbations results in a lowered opacity redward of the $H\beta$ line compared to the VCS and TB calculations. Finally, we note that our quantum electron-broadening treatment produces broader $H\beta$ and $H\gamma$ profiles for these conditions ($T_e = 1$ eV, $n_e = 10^{18}$ e/cc).

This ab initio calculation illustrates the potential power of this approach: we are able to solve for eigenstates spanning a broad range of conditions, from tightly bound and minimally perturbed to beyond the Inglis-Teller limit, all without recourse to an ad-hoc occupation-probability treatment. Besides providing a more self-consistent treatment of line profiles, this approach could lead to a parameterization of the “effective occupation probability” of different atomic states that could be incorporated into model-atmosphere and other atomic codes.

Acknowledgments. T.A.G. acknowledges support from the National Science Foundation Graduate Research Fellowship under grant DGE-1110007. M.H.M. and D.E.W. acknowledge support from the United States Department of Energy under grant DE-SC0010623.

References

- Alexiou, S., & Poquérusse, A. 2005, Phys. Rev. E, 72, 046404
- Baranger, M. 1958, Physical Review, 112, 855
- Barstow, M. A., Bond, H. E., Holberg, J. B., et al. 2005, MNRAS, 362, 1134

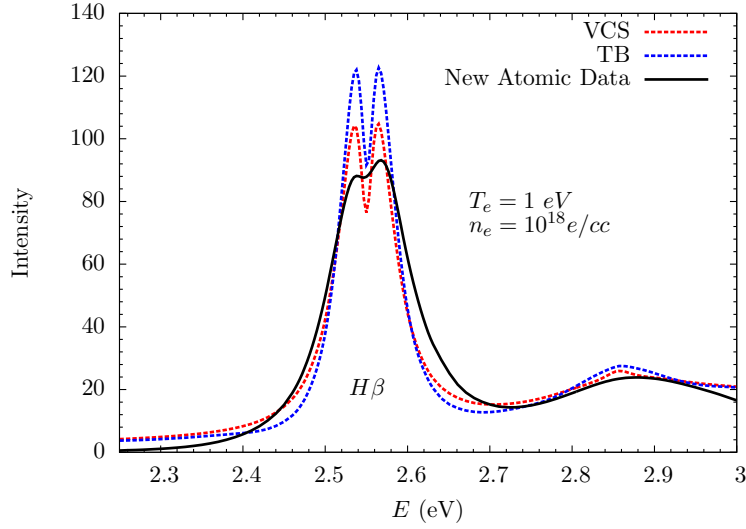


Figure 4. A preliminary comparison of VCS, TB, and our new semi-analytic profiles for a temperature of 1 eV and a density of 10^{18} e/cc.

- Barstow, M. A., Bond, H. E., Burleigh, M. R., et al. 2015, in 19th European Workshop on White Dwarfs, edited by P. Dufour, P. Bergeron, & G. Fontaine, vol. 493 of Astronomical Society of the Pacific Conference Series, 307
- Carlhoff, C., Krametz, E., Schaefer, J. H., & Uhlenbusch, J. 1986, J. Phys. B: At., Mol. Opt. Phys., 19, 2629
- Catalán, S., Isern, J., García-Berro, E., & Ribas, I. 2008, MNRAS, 387, 1693
- Crowley, B. J. B. 2014, High Energy Density Physics, 13, 84
- Dappen, W., Anderson, L., & Mihalas, D. 1987, ApJ, 319, 195
- Djurović, S., Čirišan, M., Demura, A. V., Demchenko, G. V., Nikolić, D., Gigosos, M. A., & González, M. Á. 2009, Phys. Rev. E, 79, 046402
- Fano, U. 1963, Physical Review, 131, 259
- Ferri, S., Calisti, A., Mossé, C., et al. 2014, Atoms, 2, 299.
- García-Berro, E., Torres, S., Althaus, L. G., Renedo, I., Lorén-Aguilar, P., Córscico, A. H., Rohrmann, R. D., Salaris, M., & Isern, J. 2010, Nat, 465, 194
- Gomez, T. A., Nagayama, T., Kilcrease, D. P., Montgomery, M. H., & Winget, D. E. 2016, Phys. Rev. A, 94, 022501
- Hubeny, I., Hummer, D. G., & Lanz, T. 1994, A&A, 282, 151
- Hubeny, I., & Lanz, T. 1995, ApJ, 439, 875
- Hummer, D. G., & Mihalas, D. 1988, ApJ, 331, 794
- Inglis, D. R., & Teller, E. 1939, ApJ, 90, 439
- Luc-Koenig, E., & Bachelier, A. 1980, J. Phys. B: At., Mol. Opt. Phys., 13, 1743
- Seaton, M. J. 1990, J. Phys. B: At., Mol. Opt. Phys., 23, 3255
- Tremblay, P., & Bergeron, P. 2009, ApJ, 696, 1755
- Tremblay, P.-E., Ludwig, H.-G., Steffen, M., Bergeron, P., & Freytag, B. 2011, A&A, 531, L19
- Tremblay, P.-E., Ludwig, H.-G., Steffen, M., & Freytag, B. 2013, A&A, 559, A104
- Uhlenbusch, J., & Viell, W. 1989, Contributions to Plasma Physics, 29, 459
- Vidal, C. R., Cooper, J., & Smith, E. W. 1973, ApJS, 25, 37
- Williams, K. A., Bolte, M., & Koester, D. 2009, ApJ, 693, 355
- Winget, D. E., Hansen, C. J., Liebert, J., van Horn, H. M., Fontaine, G., Nather, R. E., Kepler, S. O., & Lamb, D. Q. 1987, ApJ, 315, L77